

Phase-Shift Analysis of Heavy-Ion System Near the Coulomb Barrier

Moon Hoe CHA and Byung Ki LEE

Department of Physics, Kangwon National University, Chunchon 200-701

Yong Joo KIM

Department of Physics, Cheju National University, Cheju 690-756

(Received 21 March 1997)

A phase shift analysis of the elastic-scattering angular distributions for the $^{16}\text{O}+^{63}\text{Cu}$ system ranging from $E_{\text{lab}}=39$ to 64 MeV is presented within the parametrized phase-shift model and the generalized Fresnel model. The observed data were well reproduced by the parametrized phase-shift model. The strong absorption radii exhibit a gradual decrease from 10.74 fm to 9.520 fm as the energy increases from 39 MeV to 64 MeV. The total reaction cross sections are also deduced at these energies.

Recently, very accurate measurements of the elastic angular distributions of $39 \text{ MeV} \leq E_{\text{lab}} \leq 64 \text{ MeV}$ ^{16}O scattered from ^{63}Cu were performed [1] at Instituto de Física da Universidade de São Paulo (IFUS). The elastic scattering data were analyzed within the framework of the algebraic potential. Reasonable agreements were obtained between the calculated results and the observed data.

In previous papers [2-4], a semiclassical phase-shift analysis based on the parametrized phase-shift model (PPSM) [5] was presented. It was applied satisfactorily for the high-energy heavy-ion systems at $E_{\text{lab}}/A=35$ MeV/nucleon. In this paper, we shall extend the use of the PPSM and its extreme classical formulation, the generalized Fresnel model (GFM) [6-8], to low energy heavy-ion elastic scattering: the $^{16}\text{O}+^{63}\text{Cu}$ system observed by Lichtenthäler *et al.* [1].

There are several reasons for applying this model in the present circumstances. One is that the elastic differential cross sections at energies around the Coulomb barrier exhibit the characteristics of Fresnel diffraction patterns. The generalized Fresnel model is the simplest one to analyze such heavy-ion elastic scatterings with Fresnel diffraction patterns. Also the parametrized phase-shift model is an improved generalized Fresnel model, as pointed out by Charagi *et al.* [9]. Especially, the parametrized phase-shift model provides a realistic deflection function and allows, consequently, the nuclear rainbow effect observed in heavy-ion elastic scattering. Furthermore such an approach can seek to extract information on the geometrical structure of the colliding nuclei.

In the parametrized phase-shift model, the nuclear phase shift of the S -matrix is expressed as [5]

$$\delta_l = s \{1 + \exp[(l - \Lambda_1)/\Delta_1]\}^{-1} \quad (1)$$

and the the modulus as

$$|S_l| = \{1 + \exp[(\Lambda_2 - l)/\Delta_2]\}^{-1}. \quad (2)$$

In these two formulae, the grazing angular momentum Λ_2 and its related width Δ_2 may be different. The meaning of these two parameters is very simple. In the interior region of the colliding nuclei $|S_l|=0$ and outside $|S_l|=1$. A smooth transition on the nuclear surface between these two extreme values proceeds in elastic scattering. In the same way, the nuclear phase shift δ_l is constant inside the nuclei and zero outside.

In the PPSM, the strong absorption radius $R_{1/2}$ and the diffusivity d are related to the grazing angular momentum Λ_2 and angular momentum width Δ_2 through the following semiclassical relationships [10-11]:

$$\begin{aligned} \Lambda_2 &= k R_{1/2} \left(1 - \frac{2\eta}{k R_{1/2}}\right)^{1/2}, \\ \Delta_2 &= kd \left(1 - \frac{\eta}{k R_{1/2}}\right) \left(1 - \frac{2\eta}{k R_{1/2}}\right)^{-1/2} \end{aligned} \quad (3)$$

where k is the wave number and η the Sommerfeld parameter. In this model, the deflection function is given by the analytical formula

$$\begin{aligned} \theta_l &= 2 \frac{d}{dl} (\sigma_l + \delta_l) \\ &= 2 \tan^{-1} \left(\frac{\eta}{l}\right) - \frac{2s}{\Delta_1} \frac{\exp[(l - \Lambda_1)/\Delta_1]}{\{1 + \exp[(l - \Lambda_1)/\Delta_1]\}^2}. \end{aligned} \quad (4)$$

In its extreme classical formulation, the parametrized phase-shift model becomes a two-parameter model, the

so-called generalized Fresnel model. The advantage of this Fresnel model lies in its simplicity. The first parameter Λ is the grazing angular momentum which gives the quarter-point property and the second one Δ gives the width of the transition region in which the elastic scattering proceeds. The effect of Δ on the scattering amplitude is described by a function $F(\Delta x)$, defined by the Fourier transform of the derivative $D(\lambda)=dg(\lambda)/d\lambda$ in terms of the continuous variable $\lambda=l+1/2$:

$$F(\Delta x) = \int_{-\infty}^{\infty} D(\lambda) \exp[i(\lambda - \Lambda)x] d\lambda. \quad (5)$$

With the reflection function

$$g(\lambda) = \{1 + \exp[(\lambda - \Lambda)/\Delta]\}^{-1}, \quad (6)$$

we have

$$F[\Delta(\theta_g - \theta)] = \frac{\pi \Delta(\theta_g - \theta)}{\sinh[\pi \Delta(\theta_g - \theta)]} \quad (7)$$

where the grazing angle $\theta_g = 2 \tan^{-1}(\eta/\Lambda)$, which gives the quarter point property $d\sigma/d\sigma_R = 1/4$. The generalized Fresnel formula for the scattering amplitude is then given in terms of the error function $\text{erfc}(x)$ by [6]

$$\frac{f(\theta)}{f_C(\theta)} = \begin{cases} 1 - \frac{1}{2} \text{erfc}(-ue^{i\pi/4}) F[\Delta(\theta_g - \theta)] & \text{for } \theta \leq \theta_g \\ \frac{1}{2} \text{erfc}(ue^{i\pi/4}) F[\Delta(\theta_g - \theta)] & \text{for } \theta \geq \theta_g \end{cases} \quad (8)$$

where $u = (\Lambda/2 \sin \theta_g)^{1/2}(\theta - \theta_g)$. This GFM expression of the scattering amplitude is valid when the Coulomb interaction plays a dominant role. The strong absorption radius $R_{1/2}$ and the diffuseness d corresponding to Eq. (3) are given by

$$kR_{1/2} = (\Lambda^2 + \eta^2)^{1/2} + \eta, \quad kd = \frac{\Delta}{[1 + (\eta/\Lambda)^2]^{1/2}}. \quad (9)$$

The elastic differential cross-sections of a $^{16}\text{O}+^{63}\text{Cu}$ system ranging from $E_{\text{lab}}=39$ to 64 MeV have been fitted with the PPSM and its extreme classical formulation, GFM. Figure 1 shows the 12 elastic scattering angular distributions for the entire energy range of the $^{16}\text{O}+^{63}\text{Cu}$

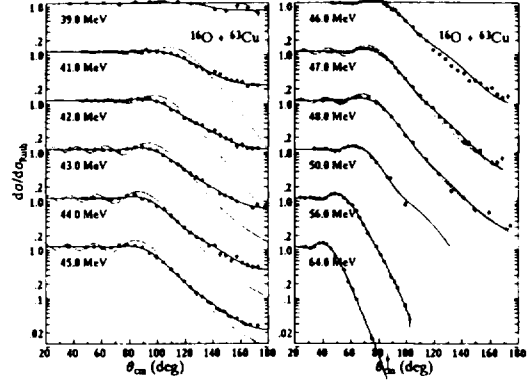


Fig. 1. Elastic angular distributions at 12 different energies for the $^{16}\text{O}+^{63}\text{Cu}$ system. The solid and dotted curves are the calculated results from the parametrized phase shift model and the generalized Fresnel model, respectively.

system near the Coulomb barrier. In this figure, we can see that the calculated results of the PPSM (solid curves) show extraordinarily good agreement with the observed data. The calculated results from the generalized Fresnel model (dotted curves) are unsuccessful as a whole and show only a diffractive Fresnel pattern. However, five GFM results at $E_{\text{lab}}=39$ MeV and $E_{\text{lab}} \geq 48$ MeV are successful with only two independent parameters; see Fig. 1 and the corresponding chi-square values listed in Table 2. The parameters of the PPSM and the GFM are given in Table 1. In this table, we can find that the grazing angular momentum Λ_1 for the nuclear phase amplitude δ_1 is much smaller than the grazing wave angular momentum Λ_2 for the $|S_l|$ modulus over the entire energy range. In Table 2, it can be seen that the strong absorption radii $R_{1/2}$ calculated from the PPSM exhibit a gradual decrease from 10.74 fm to 9.520 fm as the energy increases from 39 MeV to 64 MeV. The total reaction cross-section σ_R increases as the incident energy

Table 1. Input values for the parametrized phase-shift model and the generalized Fresnel model.

E_{lab} (MeV)	Parametrized phase shift model					Generalized Fresnel model	
	Λ_1	Δ_1	Λ_2	Δ_2	s	Λ	Δ
39	0.01	0.23	8.37	3.96	0.69	0.02	3.64
41	2.47	4.78	9.94	3.40	0.77	7.96	0.85
42	5.82	4.35	12.25	3.24	0.80	10.49	0.76
43	7.00	4.20	12.08	3.27	0.88	11.34	0.01
44	8.91	4.38	12.99	3.20	0.95	13.11	0.01
45	10.32	4.50	12.61	3.40	1.00	13.67	0.01
46	11.65	4.06	15.32	3.58	1.08	16.20	1.26
47	13.64	4.18	14.94	4.05	1.38	17.92	0.32
48	14.58	4.31	14.36	4.55	1.68	18.87	0.39
50	17.67	4.04	20.76	3.27	0.92	21.79	1.46
56	23.76	3.03	26.16	4.21	0.99	27.52	1.36
64	29.69	3.51	31.22	4.89	1.00	33.66	2.09

Table 2. Analysis results from the parametrized phase-shift model and the generalized Fresnel model.

E_{lab} (MeV)	Parametrized phase shift model					Generalized Fresnel model				
	θ_g (deg)	$R_{1/2}$ (fm)	d (mb)	σ_R (mb)	χ^2/N	θ_g (deg)	$R_{1/2}$ (fm)	d (mb)	σ_R (mb)	χ^2/N
39	180	10.74	2.58×10^{-5}	1.394	0.86	180	10.74	7.14×10^{-4}	72.41	4.36
41	168	10.25	1.15×10^{-1}	173.6	0.81	142	10.52	6.27×10^{-2}	124.9	33.8
42	152	10.14	2.41×10^{-1}	241.1	0.53	130	10.49	7.09×10^{-2}	196.6	21.8
43	145	9.979	2.75×10^{-1}	266.0	0.84	126	10.34	9.92×10^{-4}	193.5	58.6
44	136	9.897	3.55×10^{-1}	343.5	1.15	118	10.30	1.11×10^{-3}	252.6	26.7
45	129	9.807	4.12×10^{-1}	403.3	1.49	116	10.15	1.14×10^{-3}	268.5	45.2
46	123	9.732	4.08×10^{-1}	421.9	8.39	106	10.25	1.60×10^{-1}	433.0	59.2
47	115	9.749	4.71×10^{-1}	516.2	1.87	99.9	10.28	4.25×10^{-2}	457.2	10.5
48	111	9.670	5.07×10^{-1}	563.1	3.41	96.4	10.22	5.38×10^{-2}	499.5	2.99
50	98.9	9.703	5.32×10^{-1}	685.4	2.49	87.0	10.28	2.15×10^{-1}	704.4	2.99
56	78.8	9.633	4.48×10^{-1}	883.1	1.06	70.7	10.21	2.13×10^{-1}	966.6	2.20
64	63.2	9.520	5.36×10^{-1}	1174	1.86	57.0	10.14	3.29×10^{-1}	1300	4.64

increases.

A further knowledge of the situation can be gained by looking at the transmission functions, $T_l=1-|S_l|^2$, plotted in Fig. 2. In this figure, we can notice that the transmission functions of the PPSM are strikingly shifted to larger angular momenta as the incident energy increases. Such shifts raise the values of the grazing angular momentum Λ_2 corresponding to $T_l=1/2$.

The real part of the S -matrix determines the deflection function of the colliding nuclei. In Fig. 3, we find that the deflection functions obtained from the PPSM represent weak nuclear rainbow effects around $L=\Lambda_1$ over the entire energy range. Since the Coulomb interaction plays a dominant role in the low-energy scattering of heavy-ions, the nuclear effect on the deflection function for the present system appears to be small, as expected.

In conclusion, we believe that the parametrized phase-shift model is capable of reproducing the 12 elastic angular distributions for the $^{16}\text{O}+^{63}\text{Cu}$ system at $E_{lab}=39\sim 63$ MeV. In this model, the strong absorption radii exhibited a gradual decrease from 10.74 fm to 9.520 fm as the energy increased from 39 MeV to 64 MeV. On the other hand, the total reaction cross-sections increased

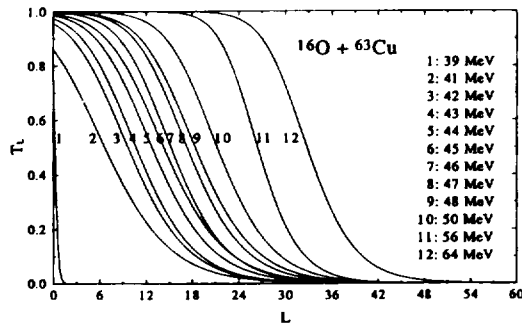


Fig. 2. Transmission functions for the $^{16}\text{O}+^{63}\text{Cu}$ system in the parametrized phase shift model plotted against the angular momentum L .

when the incident energy increased. Since the Coulomb interaction is dominant in low-energy scattering of heavy-ions, the nuclear effect on the deflection function for the present system appeared to be small as expected.

ACKNOWLEDGMENTS

It is a pleasure to thank Dr. Lichtenthaler for providing us with his beautiful data. The present study was supported by the Basic Science Research Program, Ministry of Education, Project No. 96-2402.

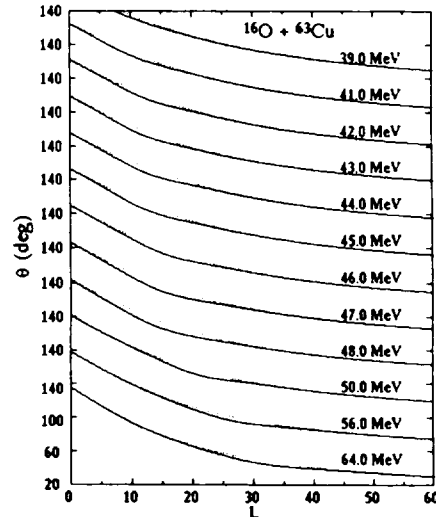


Fig. 3. Deflection functions for the $^{16}\text{O}+^{63}\text{Cu}$ system in the parametrized phase-shift model plotted against the angular momentum L . The dotted curves indicate the deflection functions for the Coulomb phase-shift only. The solid curves denote the deflection functions for the Coulomb plus nuclear phase-shifts.

REFERENCES

- [1] R. Lichtenthäler, D. Pereira, L. C. Chamon and L. C. Gomes, *Phys. Rev.* **C50**, 3033 (1994).
- [2] M. H. Cha and Y. J. Kim, *J. Phys. G: Nucl. Part. Phys.* **16**, L281 (1990).
- [3] M. H. Cha, B. K. Lee, K. S. Sim and Y. J. Kim, *J. Korean Phys. Soc.* **23**, 450 (1990).
- [4] M. H. Cha, S. K. Nam, J. Kim, B. K. Lee, M. W. Kim and K. S. Sim, *J. Korean Phys. Soc.* **24**, 299 (1991).
- [5] J. A. McIntyre, K. H. Wang and L. C. Becker, *Phys. Rev.* **117**, 1337 (1960).
- [6] W. E. Frahn, *Nucl. Phys.* **A302**, 267 (1978).
- [7] W. E. Frahn, *Nucl. Phys.* **A302**, 281 (1978).
- [8] L. N. Pandey and S. N. Mukherjee, *Phys. Rev.* **C29**, 1326 (1984).
- [9] S. K. Charagi, S. K. Gupta, M. G. Bertgeri, C. V. Fernandes and Kuldeep, *Phys. Rev.* **C48**, 1152 (1993).
- [10] M. C. Mermaz, *Z. Phys.* **A321**, 613 (1985).
- [11] M. C. Mermaz, *Il Nuovo Cimento* **88A**, 286 (1985).